frontiers | Frontiers in Marine Science

TYPE Original Research
PUBLISHED 08 December 2022
DOI 10.3389/fmars.2022.1062884

OPEN ACCESS

EDITED BY
Anthony Grehan,
University of Galway, Ireland

REVIEWED BY
Craig M. Young,
University of Oregon, United States
Alan David Fox,
Scottish Association For Marine Science, United Kingdom

*CORRESPONDENCE
Vilhelm Fagerström
vilhelm.fagerstrom@gu.se

SPECIALTY SECTION
This article was submitted to Deep-Sea Environments and Ecology, a section of the journal Frontiers in Marine Science

RECEIVED 06 October 2022
ACCEPTED 25 November 2022
PUBLISHED 08 December 2022

CITATION
Fagerström V, Broström G and Larsson AI (2022) Turbulence affects larval vertical swimming in the cold-water coral *Lophelia pertusa*. *Front. Mar. Sci.* 9:1062884. doi: 10.3389/fmars.2022.1062884

Turbulence affects larval vertical swimming in the cold-water coral *Lophelia pertusa*

Vilhelm Fagerström[1]*, Göran Broström[1] and Ann I. Larsson[2]

[1]Department of Marine Sciences, University of Gothenburg, Gothenburg, Sweden, [2]Tjärnö Marine Laboratory, Department of Marine Sciences, University of Gothenburg, Strömstad, Sweden

Vertical migration of marine larvae may drastically affect their dispersal, especially if they are spawned in the deep sea. Previous studies have shown that the planktonic larvae of the cold-water coral *Lophelia pertusa* in still water swim upwards at a speed of ca. 0.5 mm s^{-1} during a pre-competency period of 3–5 weeks. This behavioral trait is thought to benefit dispersion of larvae as it promotes near surface drift in relatively strong currents. In the ocean however, larvae regularly encounter turbulent water movements potentially impeding their swimming ability. With no apparent stabilizing mechanism, it may be expected that the body orientation of these larvae, and consequently their directed swimming, is sensitive to perturbation by external forces. We investigated the effects of turbulence on vertical swimming of pre-competent *L. pertusa* larvae by exposing them to relevant turbulence intensities within a grid-stirred tank. Larval movement and water flow were simultaneously recorded, allowing for analysis of individual larval swimming velocities. We showed that the upwards directed swimming speed generally decreased with increasing turbulence, dropping to non-significant in turbulence levels occurring near ocean boundaries. Our results do however suggest that *L. pertusa* larvae maintain their upwards directed swimming, albeit at reduced speed, in a major part of the water column, thus allowing them to spend part of their planktonic phase in the uppermost ocean layer. This new insight into the behavior of *L. pertusa* larvae in their natural environment strengthens the notion of the species as one with strong potential for long-distance dispersal. Such information is important for the understanding of *L. pertusa* population connectivity, and vital when developing tools for modelling of larval transport.

KEYWORDS

turbulence, larval behavior, planula, *Lophelia pertusa*, *Desmophyllum pertusum*, vertical migration, dispersal, particle image velocimetry

Introduction

Population connectivity in many benthic marine invertebrates is to a great extent governed by the dispersal patterns of their planktonic larvae. Dispersal patterns are in turn governed by environmental factors such as hydrodynamics and food availability, which tend to vary considerably with depth. Behavioral traits that affect the vertical distribution of larvae may therefore have a strong impact on population connectivity and population dynamics (Levin, 2006; McVeigh et al., 2017; Gary et al., 2020). Knowledge about environmental elements as well as larval behavior is therefore essential for effective and sustainable management of many marine habitats.

Framework-forming scleractinian cold-water corals are benthic marine organisms that build complex three-dimensional structures made up by their hard calcium carbonate skeleton. As the name suggests, they inhabit parts of the ocean where the water temperature is low, typically at depths below the photic zone. Provided that the environmental conditions are favorable, large numbers of individual coral colonies may form extensive reefs that provide habitat for numerous other species. These reefs constitute biodiversity hotspots in areas where diversity otherwise tends to be low. In addition to being sites of great productivity in the deep sea, cold-water coral reefs are sensitive ecosystems that in many cases have suffered extensive damage, primarily from intrusive fishing activity (Koslow et al., 2001; Fosså et al., 2002; United Nations, 2006).

Lophelia pertusa (synonym *Desmophyllum pertusum*) is the most widespread framework-forming scleractinian cold-water coral, with a near-global but scattered distribution (Rogers, 1999; Roberts et al., 2009). Reefs of *L. pertusa* may extend over several kilometers (Freiwald et al., 2004) and studies from the N.E. Atlantic have found more than 1300 species linked to these habitats (Roberts, 2006). Typically, *L. pertusa* reefs are found along continental margins, on seamounts and in fjords below the thermocline (Rogers, 1999; Roberts et al., 2003; Freiwald et al., 2004). In such areas, the species prefers locations where environmental requirements, including sufficient food supply and hard substrate for larvae to settle on, are met.

The sexual reproduction in *L. pertusa* is external and successful fertilization results in planktonic, ciliated planula larvae that are near spherical in shape and measure about 0.2 mm in diameter (Larsson et al., 2014). Body size and general shape are maintained throughout the planktonic larval phase although the shape is plastic and can shift to more elongated depending on activity, especially in older larvae (Strömberg et al., 2019). Previous observations of *L. pertusa* embryos spawned in aquaria suggest that they, as well as the developed planulae, are neutrally buoyant (Larsson et al., 2014). The density distribution across the larval body has not yet been studied in detail, but observations of larvae in culture suggest that it is uniform with the center of mass in the center of the body. *L. pertusa* planulae are planktotrophic and the pelagic larval duration for the species can last for months (Strömberg and Larsson, 2017), providing prerequisite for dispersal over large distances.

In still water, Strömberg and Larsson (2017) observed a pattern of developmental shifts in vertical migration of *L. pertusa* larvae. Pre-competent planulae were seen to possess a negative geotactic behavior, with active upwards directed helical swimming until at least 5 weeks of age. No signs of phototaxis have been observed in the species (Larsson et al., 2014). Larvae have not been seen sampling the bottom substrate before 3 weeks after fertilization and such a behavior does not appear to become more common until 4-5 weeks of age (Larsson et al., 2014). Upwards directed swimming velocities of 0.5 mm s^{-1} (43 m d^{-1}) have been recorded in pre-competent larvae, implying that they may potentially spend a substantial part of their pelagic larval duration in the near-surface water where current velocities and food abundance tend to be higher than within the ocean interior. These observations are in concert with results from biophysical modelling of *L. pertusa* larval drift, which showed closer resemblance to observed genetic structure (Dahl, 2013) when larvae moved towards the surface for the first weeks of their larval stage (Fox et al., 2016). Vertical migration, if maintained in the natural habitat, would add to the potential for long distance larval transport in the species.

Haloclines and turbulence are two examples of environmental factors known to potentially hinder the vertical migration of marine invertebrate larvae (Sameoto and Metaxas, 2008; Clay and Grünbaum, 2010; McDonald, 2012). Pre-competent *L. pertusa* larvae have been seen to cross salinity gradients in the laboratory without slowing down (Strömberg and Larsson, 2017), suggesting that salinity gradients typical of haloclines do not obstruct their upwards directed migration. Turbulence is known to inhibit or alter directed swimming in other invertebrate larvae, by tilting them away from their stable axis and/or induce behavioral changes (Jonsson et al., 1991; Grünbaum and Strathmann, 2003; Fuchs et al., 2004; Clay and Grünbaum, 2010; McDonald, 2012; Wheeler et al., 2013; Fuchs et al., 2015).

Oceanic turbulence is often quantified based on the dissipation rates, ϵ, of turbulent kinetic energy, which typically ranges from 10^{-10} to 10^{-4} m^2 s^{-3} (numbers presented in e.g., Kiørboe and Saiz, 1995; Fuchs and Gerbi, 2016; Franks et al., 2022). Turbulence is generally weak ($\epsilon \leq 10^{-8}$ m^2 s^{-3}) away from ocean boundaries and stronger (ϵ up to 10^{-4} m^2 s^{-3}) near the sea surface or near the sea floor. Vertically migrating planktonic larvae may consequently experience turbulence with ϵ ranging over several orders of magnitude.

Here we describe the effect of turbulence on the active vertical swimming of pre-competent *L. pertusa* planulae. The objective of the study was to gain understanding about the influence of oceanic turbulence on *L. pertusa* larval dispersal. We pursued this objective by studying the organism in a laboratory

environment, exposing pre-competent larvae to relevant levels of turbulence within a grid-stirred tank. Our main hypothesis states that the upwards directed swimming in *L. pertusa* larvae is negatively affected by turbulence and that there is an upper intensity threshold above which the behavior is no longer sustained. We base this hypothesis on the argument that turbulence will cause disruption to the preferred orientation of swimming larvae and that the level of disruption increases with the turbulence. The experiments were thus carried out with the expectation that larvae would demonstrate upwards directed swimming in still water and in weak turbulence, while such movement would be reduced or absent for larvae in stronger turbulence.

To our knowledge, this is the first study of the effects of turbulence on swimming in any Cnidarian planulae and/or larvae of any deep-sea organism. Previous studies addressing effects of turbulence on the behavior of marine invertebrate larvae have focused on organisms that have some means of passively directing them in relation to the vertical, such as a center of gravity located away from the center of the body while swimming (Jonsson et al., 1991; Fuchs et al., 2004; Wheeler et al., 2013; Fuchs et al., 2015). In contrast, the body characteristics of *L. pertusa* larvae do not offer them any obvious aid in passively maintaining their orientation. It may therefore be expected that these larvae are more sensitive to disruptive forces (McDonald, 2012) and thus less prone to active vertical migration when exposed to turbulence. This, in combination with modelling results indicating a potentially significant impact of vertical migration on *L. pertusa* larval transport, makes it highly relevant to assess the effects of turbulence on the swimming behavior of these organisms.

Materials and method

Coral collection and larval culturing

Lophelia pertusa coral samples were collected from the Tisler reef located in the Ytre Hvaler National Park (NE Skagerrak). Collection took place on December 3rd, 2018, using a remotely operated vehicle (ROV, Ocean Modules V8 Sii). All necessary permits were in place (see Supplementary Information section 1). The corals were sampled from colonies at 100 – 120 m water depth. Collected samples were brought to the Tjärnö Marine Laboratory, University of Gothenburg, where the sex of each sample was determined through dissection of polyps. The corals were distributed, mixing male and female fragments, into six 18-L tanks connected to a piping system, allowing flow through of 50 µm filtered sea water with a salinity of 30.3 – 34.5 g kg^{-1} and a temperature of 7 – 8°C. The corals were fed twice a week with frozen zooplankton.

Larvae for this study were produced during three spawning events, on February 14th, 15th and 23rd, 2019. The three larval batches are hereafter referred to as B1, B2 and B3 respectively, numbered with respect to the chronology of spawning dates. Spawned egg and sperm were collected from the tanks and kept in 3 L glass jars for 2 – 3 days. The developed embryos were subsequently transferred into 5 µm filtered seawater in 2-L Erlenmeyer flasks. Larvae were cultured at 8°C and densities of 0.5 – 1.0 larvae mL^{-1}, until the experiments were carried out on March 5th, 6th and 14th for B1, B2 and B3 respectively. The larvae were 19 days old when tested and were, by then, fully developed swimmers, striving upwards in the water column. Based on observations reported by Larsson et al. (2014) and by Strömberg and Larsson (2017), we assume that larvae were swimming at their maximum speed at the time of the experiments. Pre-competency was considered probable based on the upwards swimming behavior and lack of cnidocytes required for attachment to surfaces (Strömberg et al., 2019). Larvae at this age have not yet a fully developed mouth, meaning that they are not yet able to ingest food particles (Strömberg and Larsson, 2017).

Grid-stirred tank and PIV system

A grid-stirred Plexiglas® tank with dimensions 32 cm × 32 cm × 70 cm (width × depth × height) was specifically constructed for the experiments (Figure 1A). The front and side walls of the tank were transparent while the back wall and bottom plate were opaque black. During the experiments, the water height was 67 cm in the tank. A transparent Plexiglas® lid covered the upper water surface. Turbulence was generated by two horizontally oriented Plexiglas® grids (Figure 1B), oscillating jointly with an amplitude of 5 cm along the vertical dimension. Grid mesh size was 32 mm (Figure 1C) and the bars of the grid had a square 8 mm × 8 mm cross section. The outer ends of the grids were "open" with the bars extending 15.5 mm from the outermost bar-crossings. The two grids were mounted 30 cm apart, equidistantly in relation to the center of the water column. Narrow steel rods, 8 mm in diameter, were connected to the corner bar-crossings of the grids as well as to a DC stepping motor (VEXTA, model BLUM440-GFS, Oriental Motor Co. Ltd. Japan) which generated the oscillating motion. Grid oscillation frequency was adjusted by a motor driver (VEXTA, model BLUD40C). All experiments were carried out in a thermo-regulated space where the ambient temperature was kept at 8.0 – 8.5°C. Water temperature during the trials was 8.1 – 8.3°C and the salinity was 33.2 – 34.0 g kg^{-1}.

Flow velocities within the tank were measured using particle image velocimetry (PIV). The PIV system from LaVision (Germany) consisted of a 1600 × 1200 pixel camera (Imager Pro X with a 50 mm Nikkor lens) and a double pulsed Nd : YAG laser (Quantel Evergreen 70, 70 mJ at 532 nm). The system allowed for single frame- or double frame capture at a maximum frequency of 15 Hz. During single frame capture, the system captures single image frames at a set frequency. Double frame

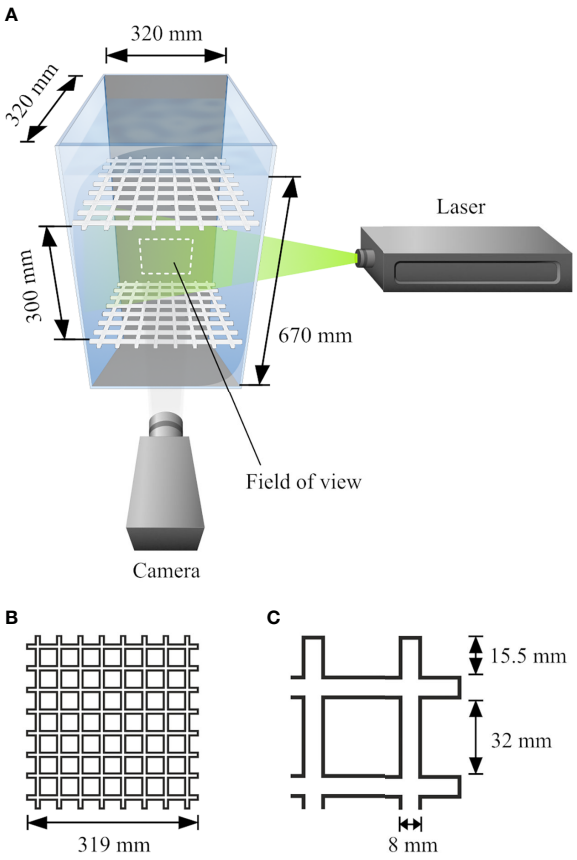

FIGURE 1
Experimental set-up for the experiments on *Lophelia pertusa* larval swimming in turbulence. **(A)** The two horizontal grids oscillate vertically to generate turbulent flow. The camera and the laser are mounted perpendicularly, capturing images with the camera field of view in the center of the water mass. **(B, C)** show the geometry of the oscillating grids.

capture implies that pairs of image frames are captured at a set frequency, with a very short time in between frames within pairs. Flow velocities may be calculated from particle displacement between paired images collected using single frame capture or from particle displacement between frames within image pairs collected during double frame capture. Neutrally buoyant hollow glass spheres (HGS–10, Dantec Dynamics), with an average diameter of 10 µm, were used as tracer particles at a concentration of about 7.5×10^3 particles mL^{-1}.

The laser was mounted to the side of the tank (Figure 1A), emitting a 1 mm thick laser sheet aligned with the center of the water column. The camera, mounted horizontally perpendicular to the laser, had a field of view (FOV) with a spatial extent of 86.3 mm × 64.8 mm, fixed in the center of the water mass. The process of finalizing the experimental setup involved testing the system with several alternative grid separation distances and FOV sizes. The chosen settings were proven to produce relevant levels of turbulence while keeping the secondary flow low and, at the same time, allowing larvae to be identified and tracked within the FOV. Due to technical limitations of the PIV system, separate experiments were required for the two purposes of estimating turbulence and study larval swimming.

Estimation of turbulence

Four turbulence levels, hereafter referred to as T_1, T_2, T_3 and T_4, were generated by oscillating the grids at frequencies of 0.045 Hz, 0.4 Hz, 0.8 Hz and 1.18 Hz respectively. Estimations of turbulent energy dissipation rates, ϵ, were based on two sets of PIV measurements for each turbulence level. All individual PIV recordings made for this part of the study were proceeded by a 10-minute resting period and a 10-minute spin-up period. Each set of PIV measurements lasted 10 minutes.

PIV velocity vector fields (see Figure S1 for examples) and velocity gradient scalar fields were calculated using cross-correlation in the DaVis (version 8.4) software from LaVision. Image pairs were processed to calculate velocity vectors u and w in the horizontal (x) and vertical (z) direction respectively. For details on PIV data processing, see Supplementary Information section 2. The turbulent energy dissipation rates were estimated directly from velocity gradient scalar fields, assuming the flow being axisymmetric about the vertical axis (z-dimension) as in George and Hussien (1991):

$$\epsilon(x,z) = \nu\left[8\overline{\left(\frac{\partial u}{\partial x}\right)^2} - \overline{\left(\frac{\partial w}{\partial z}\right)^2} + 2\overline{\left(\frac{\partial u}{\partial z}\right)^2} + 2\overline{\left(\frac{\partial w}{\partial x}\right)^2}\right] \quad \text{(Equation 1)}$$

where ν is the kinematic viscosity. The two-dimensional components of the strain rate tensor are time-averaged over the timespan of the PIV recording.

Larval vertical swimming experiments

Swimming in still water

Still water swimming experiments were run in tanks with dimensions 15 cm × 10 cm × 50 cm, filled to a water height of 25 cm. Water temperature and salinity during trials were 8°C and 33 – 34 g kg^{-1} respectively. To determine the effect of added PIV seeding particles on the vertical larval swimming velocity, experiments with and without seeding particles were conducted for larvae from B1 and B2. For larvae from B3, still water experiments were only performed in water without seeding particles due to a lower number of available larvae. For the trials involving water containing seeding particles, a concentration of about 7.5×10^3 particles mL^{-1} was used.

The swimming of 17–26 larvae was recorded for each treatment and larval batch (Table 1). Approximately half of all available larvae from a batch were initially added and recorded. After removal of the

larvae initially added. the procedure was repeated with the remaining half. The larvae were introduced 2 cm above the bottom of the tank using a pipette and swimming was recorded for 13 – 15 minutes with a Canon EOS 5D Mark II camera. The tanks were illuminated by light sources mounted laterally on either side and the camera field of view covered the full vertical and horizontal extent of the water column. Larval swimming was recorded by collection of image sequences from which individual larvae were manually tracked using the software plugin MTrackJ (version 1.5.1) (Meijering et al., 2012) within the ImageJ software (version 1.52a) (Schneider et al., 2012). Vertical swimming velocities were estimated from vertical larval displacement between image frames, 10 s apart, assuming negligible advection.

Swimming in turbulence

One trial comprising all four turbulence levels was conducted for each of the three larval batches. Trials were initiated by letting the grids oscillate at the lowest frequency of 0.045 Hz for 10 minutes to allow build-up of fully developed turbulence within the tank. Larvae were added to the tank from above, using a 25 mL bulb pipette. The larvae were introduced below the FOV, approximately 2.5 cm above the highest position of the lower grid. Treatment T_1 was conducted first during each trial while subsequent treatments were randomly ordered. This strategy was chosen to maximize the number of larvae initiating their swimming below the FOV, as most larvae were expected to maintain upwards swimming in this treatment while down-mixing was expected to be low. After each change in oscillation frequency, turbulence was allowed to establish for 10 minutes before recording of larval swimming begun.

All available larvae were used for the experiments. In trials testing larvae from B1 and B2, approximately half of the larvae were introduced after the initial 10-minute spin-up of the tank while the remaining larvae were added after completion of treatment T_1. For the trial testing larvae from B3, all larvae were introduced after the initial 10-minute spin-up of the tank and no larvae were added thereafter. This inconsistency was due to a lower number of larvae in B3, necessitating the inclusion of all larvae during T_1.

Image sequences were collected by manually triggering the PIV system to capture frames for a duration of 10 – 13 s whenever suspected larvae were observed within the FOV. Particles with a documented diameter of 0.16 – 0.27 mm and a regular, near spherical shape were assumed to be larvae and image sequences containing such particles were selected for further analysis. The chosen criteria were based on known larval size as well as the observed appearance in image sequences from T_1 where larvae were identified with great confidence by their upwards directed helical swimming.

As for the still water swimming experiments, larvae recorded in turbulence were manually tracked using the MTrackJ plugin for ImageJ. Some of the recorded larvae remained illuminated by the laser sheet in the FOV for a very short time and a minimum track length of 5 frames was set as a criterion for inclusion in the subsequent analysis. This criterion resulted in a total of 117 analyzed larval trajectories across all turbulence levels and batches. The numbers of analyzed trajectories for each larval batch and treatment are presented in Table 2.

The vertical component, w_l, of the two-dimensional larval movement was calculated from vertical larval displacement between frames. The vertical component, w_S, of the two-dimensional swimming speed of individual larvae was estimated by subtracting the corresponding component, w_f, of the local water flow velocity from w_l:

$$w_s = w_l - w_f \quad \text{(Equation 2)}$$

Local vertical flow velocities were estimated through unweighted linear interpolation of the measured flow velocities to individual larval positions. The performance of the interpolation procedure was evaluated by comparing interpolated velocities to measured velocities in datasets without larvae. Our method for isolating the vertical larval swimming velocity is similar but not equal to those used by (Wheeler et al. 2013 and Wheeler et al 2016).

Deteriorated PIV estimates were occasionally observed in the immediate vicinity of individual larvae. Exclusion of velocity vectors within a distance corresponding to the sum of the maximum larval radius and 1.5 times the grid size of the vector field was seen to reduce the influence by these spurious estimates while limiting interpolation errors caused by excess removal of vectors. Remaining flow velocity vectors were interpolated into each recorded larval position (Figure 2) and the interpolated velocities were subsequently averaged for each larval trajectory segment (similar to Fuchs et al., 2013). This procedure resulted in the w_f which was subtracted from w_l to estimate w_s.

Due to unequal lengths of larval trajectories, all statistical analyses were done on trajectory averages, $\langle w_s \rangle_{Tr}$, of estimated vertical swimming velocities. Individual $\langle w_s \rangle_{Tr}$ resulted from averaging of Equation 2 over the entire lengths of individual larval trajectories:

$$\langle w_s \rangle_{Tr} = \langle w_l - w_f \rangle_{Tr} \quad \text{(Equation 3)}$$

One estimate of $\langle w_s \rangle_{Tr}$ was calculated for each larval trajectory and hence for each of the observed larvae, assuming a negligible risk of recording individual larvae more than once.

Statistical analyses

The effect of PIV particles and larval batch on vertical swimming velocity in still water was analyzed with a two-way

TABLE 1 The number of *Lophelia pertusa* larvae tracked during the still water swimming experiments, categorized by larval batch and experimental treatment.

	B1	B2	B3
No seeding particles	20	21	26
Seeding particles	17	22	

unbalanced ANOVA using Type-III sums of squares. Both factors were considered fixed. Normal distribution and equal variances of the data were indicated by visual assessment and supported by results from Shapiro-Wilk tests and Levene's test respectively.

The main objective of the turbulence experiments was to identify possible effects of turbulence on vertically directed swimming of pre-competent *L. pertusa* larvae. The null hypothesis, stating that $\langle w_s \rangle_{Tr} = 0$, was tested for each combination of turbulence level and larval batch using two-tailed one-sample t-tests. Statistical tests were not applied across turbulence levels. Results from Shapiro-Wilk tests supported normal distribution of data from each group tested except for batch B3 in treatment T_4 [$W_{B3,T4} = 0.778$, $p_{B3,T4} = 0.025$]. For this treatment the non-parametric Wilcoxon signed rank test was performed instead of a two-tailed one-sample t-test. All statistical tests were done in R (R Core Team, 2020) using built in functions as well as the packages *car* (Fox and Weisberg, 2019) and *lawstat* (Gastwirth et al., 2019). A significance level $\alpha = 0.05$ was used throughout.

Results

Turbulent energy dissipation rates

Turbulence in the grid-stirred tank increased with grid oscillation frequency (Table 3) and estimated turbulent kinetic energy dissipation rates, ϵ, ranged from 9.03×10^{-9} to 1.05×10^{-5} m^2 s^{-3}. Temperature and salinity during trials were 8.3°C and 33.3 g kg^{-1} respectively, resulting in a kinematic viscosity, ν, of 1.42×10^{-6} m^2 s^{-1}. Corresponding Kolmogorov length scales, $\eta = (\nu^3/\epsilon)^{1/4}$, were 0.72 – 4.22 mm, implying that the distance, Δx, between PIV vector grid nodes was smaller than the size of the smallest energy containing eddies at all turbulence levels.

The estimated ϵ for set grid oscillation frequencies varied both spatially within the FOV and in-between trials (Table 3, Figure S2). For turbulence treatment T_4, the estimated in-between trials difference of ϵ was high and comparable to the difference in average ϵ between turbulence treatment T_3 and T_4. For T_1 through T_3, the in-between trials differences as well as the spatial variation of ϵ were small in relation to the relative differences of ϵ between turbulence treatments.

Larval swimming in still water

The two-way ANOVA revealed no significant differences in trajectory averaged vertical swimming velocity, $\langle w_s \rangle_{Tr}$, for any of the main factors, i.e., presence of PIV seeding particles [$F_{(1,76)} = 0.06$, $p = 0.81$] or larval batch [$F_{(1,76)} = 0.63$, $p = 0.43$]. The interaction between the factors PIV particles and larval batch was significant [$F_{(1,76)} = 4.11$, $p = 0.046$] because of opposite reactions to the presence of PIV particles for the two larval batches (Figure 3). Larvae in B1 swam on average slower and larvae in B2 on average faster with added PIV particles. Thus, no general effect of the presence of PIV particles on larval vertical swimming performance could be detected.

TABLE 2 Results from one sample t-tests and non-parametric Wilcoxon signed rank test*, testing the null hypothesis of trajectory averaged vertical swimming velocity, $\langle w_s \rangle_{Tr}$, being equal to zero in *Lophelia pertusa* larvae.

Treatment	Batch	Number of trajectories	One sample t-test /Wilcoxon signed rank test*	
			t/V*	p-value
Still water	B1	20	17.69	**<0.001**
	B2	21	14.75	**<0.001**
	B3	26	16.60	**<0.001**
T_1	B1	14	7.95	**<0.001**
	B2	18	10.70	**<0.001**
	B3	5	17.38	**<0.001**
T_2	B1	18	9.22	**<0.001**
	B2	11	3.96	**0.003**
	B3	7	2.95	**0.026**
T_3	B1	8	−0.95	0.373
	B2	7	−0.22	0.830
	B3	8	−1.37	0.213
T_4	B1	5	−1.34	0.252
	B2	9	0.65	0.532
	B3	7	1*	**0.031***

Treatments included still water and four turbulence levels denoted T1–T4, numbered by increasing turbulence. Significant p-values are displayed in bold (significance level $\alpha = 0.05$)

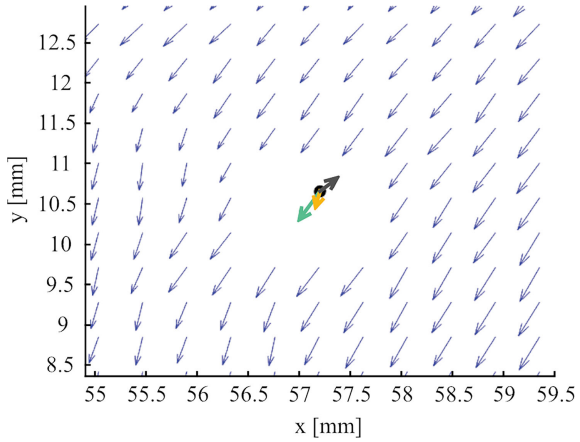

FIGURE 2
Example image from measurements of larval swimming in the grid-stirred tank showing local flow field vectors calculated using PIV (blue) with vectors removed near the larva (black marker), flow vector interpolated in larva location (turquoise), larval movement vector (yellow) and calculated instantaneous larval swimming vector (dark grey).

The $\langle w_s \rangle_{Tr}$ estimated for larvae in still water without PIV seeding particles will hereafter be referenced to when comparing with $\langle w_s \rangle_{Tr}$ estimated in turbulence treatments. The no-particle estimates are used to allow still water comparison for all three larval batches. In still water, the mean $\langle w_s \rangle_{Tr}$ was 0.36 ± 0.11 mm s^{-1} (mean ± SD) across batches (Figure 4).

Vertical swimming velocity in turbulence

Larval swimming in the grid-stirred tank changed with ϵ (Figure 4, Table 2). The statistical tests indicate that $\langle w_s \rangle_{Tr}$ remained significantly positive (directed upwards) in turbulence levels T_1 and T_2 for all three larval batches (Table 2). Across-batch averages of $\langle w_s \rangle_{Tr}$ decreased by 24.8% and 30.0% in T_1 and T_2 respectively, compared to $\langle w_s \rangle_{Tr}$ estimated from still-water trials (Figure 4). In the two highest turbulence levels, T_3 and T_4, $\langle w_s \rangle_{Tr}$ did not differ significantly from zero, except for those estimated from B3 in T_4 for which $\langle w_s \rangle_{Tr}$ were significantly negative (Table 2). More detailed statistics on larval swimming are given in Table S1.

Discussion

With near spherical bodies, neutral buoyancy and no apparent offset between center of mass and center of body, planula larvae from the cold-water coral *Lophelia pertusa* have no obvious, passive mechanism that directs their body. It may thus be expected that their body orientation, and consequently their directed swimming, is sensitive to perturbation by external forces (McDonald, 2012). Our results show that these larvae do nonetheless maintain upwards directed swimming in turbulence typical of the ocean interior (Fuchs and Gerbi, 2016; Bendtsen and Richardson, 2018; Franks et al., 2022). However, in turbulence with elevated intensity, such as that encountered at ocean boundary layers, larvae appear to lose this propensity (Figure 4; Table 2).

Our hypothesis, stating that upwards directed swimming in *L. pertusa* larvae is negatively affected by turbulence and that there is an upper turbulence threshold for the occurrence of the trait, is thus supported by the results. Our observations suggest that the larvae do indeed migrate vertically through a major part of the oceanic water column and likely reach the upper ocean where they may reside during a substantial part of their larval period. These findings are of great importance as vertical migration of larvae appears to have a strong impact on both the direction and distance of their dispersal (e.g., Fox et al., 2016; McVeigh et al., 2017; Gary et al., 2020).

Methodology – Grid-stirred tank and estimation of larval swimming

Adjusting the grid oscillation frequency, we generated turbulence with turbulent kinetic energy dissipation rates, ϵ, between 9.03×10^{-9} and 1.05×10^{-5} m^2 s^{-3} in the grid-stirred tank (Table 3). The corresponding Kolmogorov length scales, η, ranged between 0.73 and 4.24 mm, implying that the spatial resolution, Δx = 0.43 mm, of the PIV velocity vector fields was consistently smaller than η. Elevated uncertainty in the estimations of ϵ with decreased turbulence level should be considered, due to the increased risk of estimation errors caused by noise as η increase in relation to Δx (Saarenrinne and Piirto, 2000; Tanaka and Eaton, 2007). By ensuring that the

TABLE 3 Summary of turbulence characteristics in the grid-stirred tank.

Turbulence level	Grid oscillation frequency (Hz)	Trial 1		Trial 2		Average	
		ϵ ($m^2 s^{-3}$)	η (mm)	ϵ ($m^2 s^{-3}$)	η (mm)	$\langle\epsilon\rangle$ ($m^2 s^{-3}$)	$\langle\eta\rangle$ (mm)
T_1	0.045	9.03×10^{-9}	4.22	1.04×10^{-8}	4.07	9.71×10^{-9}	4.14
T_2	0.4	1.92×10^{-7}	1.97	2.21×10^{-7}	1.90	2.07×10^{-7}	1.93
T_3	0.8	2.26×10^{-6}	1.06	2.30×10^{-6}	1.06	2.28×10^{-6}	1.06
T_4	1.18	1.05×10^{-5}	0.72	6.13×10^{-6}	0.83	8.32×10^{-6}	0.77

density of PIV seeding particles was sufficient and by adjusting the Δt between frames for optimal particle displacement, the risk for spurious vectors was reduced.

Variations of estimated ϵ, both spatially and in-between trials, indicate some degree of inhomogeneity of the turbulence in the central part of the grid-stirred tank (Table 3; Figure S1). Such variations must be acknowledged when interpreting the results since they translate into variation in the turbulence experienced by observed larvae. They do not, however, undermine our possibilities to assess the directed swimming in turbulence since larvae were tracked from all parts of the FOV and during three trials per turbulence level.

We noted that the variation in estimated trajectory averaged vertical swimming velocities, $\langle w_s \rangle_{Tr}$, increased with turbulence (Figure 4; Table S1). This may partly be explained by the increased spatial variance of the flow velocities generated within the grid-stirred tank. Such an increase may alter the range of water motion experienced by individual larvae, but moreover it will add uncertainty to the interpolation of flow velocities into larval positions. Interpolation performance tests showed that errors tend to increase with increasing turbulence, although the average difference between interpolated and measured vertical velocities was close to zero for all turbulence treatments. Interpolation errors of this kind do therefore not disallow assessment of larval swimming along the vertical axis.

Our hypothesis was based on the on the argument that turbulent water movements would repeatedly tilt swimming larvae away from their preferred orientation. Larvae swimming with constant speed but in random directions would lead to a decrease in their mean absolute w_s and an increase in the variation. The data is thus consistent with this argument, but the turbulence-dependent uncertainty of the velocity interpolation procedure implies that we cannot make rigorous conclusions regarding speed or directionality of larval swimming in higher turbulence. Our results concerning the influence of turbulence on the vertical swimming in *L. pertusa* larvae remain solid even though the mechanism/s causing the observed effect could not be identified. A reduction in vertical swimming speed may indeed be attributed to a loss of orientation as suggested by the hypothesis, but it may alternatively be caused by e.g., a reduced swimming activity or a combination of disturbance and altered behavior.

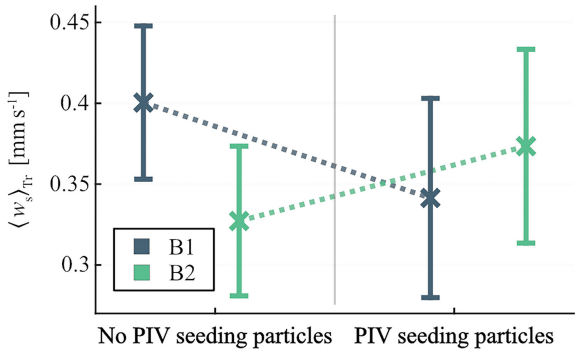

FIGURE 3
Mean trajectory averages, $\langle w_s \rangle_{Tr}$, of estimated vertical swimming velocity in still water, with and without PIV seeding particles. Colors indicate *Lophelia pertusa* larval batch and error bars represent 95% confidence intervals.

Larval swimming in turbulence and implications for dispersal and settlement

Our experiments were designed to appropriately address the question of how vertical swimming in *L. pertusa* larvae may be affected by turbulence that they encounter during their pelagic phase. The turbulence intensities to which larvae were exposed in the experiments were therefore intended to be comparable to those encountered in the water column of the open ocean. Field measurements have shown that ϵ of the open ocean typically range between 10^{-11} and 10^{-4} m^2 s^{-3} (e.g., Kiørboe and Saiz, 1995; Fuchs and Gerbi, 2016; Bendtsen and Richardson, 2018; Franks et al., 2022). Corresponding η between 13 and 0.4 mm imply that the smallest energy containing eddies of marine turbulent flows are commonly larger or much larger than the size of *L. pertusa* planulae. This suggests that *L. pertusa* larvae are likely to experience turbulence as temporally varying sub-microscale shear in their natural environment.

Below the mixed layer, away from ocean boundaries, ϵ is commonly very low, reflecting weak turbulent mixing, while turbulence may be elevated by several orders of magnitude near boundaries. In a data synthesis presented by Franks et al. (2022), the authors found median ϵ of about 10^{-10} m^2 s^{-3} below 100 m depth while rates higher than 10^{-8} m^2 s^{-3} rarely occur below 150 m. Dissipation rates higher than 10^{-7} m^2 s^{-3} were reported as uncommon between 50 and 20 m depth whereas values between 10^{-6} and 10^{-5} m^2 s^{-3} are reached during brief events, lasting 10 min or less.

Although not covering the entire span of ϵ observed in the ocean, those generated within the grid-stirred tank were shown to be relevant to the objective of our study. Ranging from roughly 10^{-8} m^2 s^{-3} to 10^{-6} m^2 s^{-3}, they compared to ϵ closer to the upper end of the spectrum encountered in the open ocean. Larval vertical swimming was affected by the generated turbulence, with trajectory averages, $\langle w_s \rangle_{Tr}$, of upwards directed swimming speed decreasing with increasing ϵ. In turbulence with dissipation rates of roughly 10^{-8} and 10^{-7} m^2 s^{-3}, $\langle w_s \rangle_{Tr}$ were decreased by 22% and 39% respectively, compared to $\langle w_s \rangle_{Tr}$ estimated for larvae swimming in still water (Figure 4). Over this interval, where ϵ increased by one order of magnitude, there was only a small reduction of $\langle w_s \rangle_{Tr}$, from 0.28 to 0.22 mm s^{-1}. In turbulence with $\epsilon \geq 2.28 \times 10^{-6}$ m^{2}s^{-3}, upwards directed swimming was not observed. When exposed to such turbulence, $\langle w_s \rangle_{Tr}$ were not significantly different from zero except for those estimated from B3 in T_4 for which significant, relative downward movement was observed.

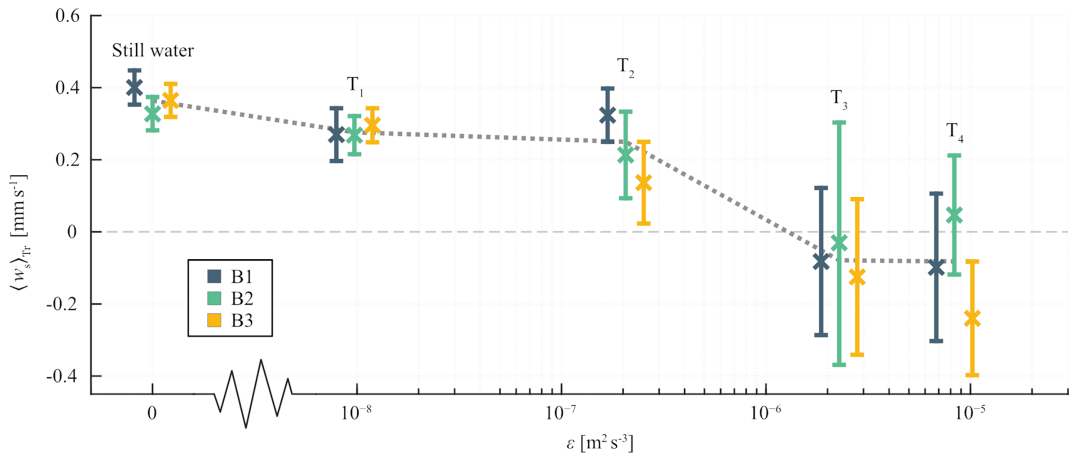

FIGURE 4
Mean trajectory averages, $\langle w_s \rangle_{Tr}$, of vertical swimming velocity in *Lophelia pertusa* larvae for different turbulent energy dissipation rates, ϵ. Error bars represent 95% confidence intervals. Colors represent larval batches, and the dotted line indicates mean values of $\langle w_s \rangle_{Tr}$ for all larvae tracked in each treatment.

The average vertical swimming velocity of 0.36 mm s^{-1}, recorded for 19-days-old larvae in our still water experiments, is lower than the 0.48 mm s^{-1} previously recorded for a batch of 27-days-old planulae in the same temperature (Strömberg and Larsson, 2017). Differences between methods, larval age and/or larval batches may explain the discrepancy. Larsson et al. (2014), measured horizontal swimming velocities in short sequences under a dissecting microscope at 8–9°C and registered 0.23, 0.51 and 0.53 mm s^{-1} for 7-, 14- and 21-days-old larvae respectively. These observations indicate that one week old larvae are still not fully developed swimmers while 2 weeks old larvae are. Besides the age of larvae, ambient temperature may affect swimming speed. Brooke and Young (2003) noted that swimming speed approximately doubled between 5 and 15°C for planulae of *Oculina varicosa*, which are of the same size as *L. pertusa* planulae. Since *L. pertusa* is a cosmopolitan species found at low to high latitudes and at various depths, its larvae may encounter a large range of temperatures. Adult corals of this species typically thrive at 4–12°C (Rogers, 1999), but water temperatures above their benthic habitats can be very different. Predictions of larval swimming and larval dispersal in *L. pertusa* are further complicated by the temperature dependent larval development (Strömberg and Larsson, 2017). These complications suggest that relative measures of the effect of turbulence on vertical swimming speed can be more helpful than absolute numbers.

Vertical swimming velocities were positive in turbulence treatment T_1 and T_2 (Figure 4), suggesting that pre-competent *L. pertusa* larvae perform vertical migration throughout most of the oceanic water column where turbulence is typically weak to moderate ($\epsilon \leq 2.07 \times 10^{-7}$ m^2 s^{-3}). In T_1, where $\epsilon \approx 10^{-8}$ m^2 s^{-3}, the average $\langle w_s \rangle_{Tr}$ was roughly 0.3 mm s^{-1}. Neglecting possible effects of temperature, such a velocity translates to a vertical swimming rate of approximately 26 m d^{-1}. Active locomotion may thereby enable larvae from most known reefs to reach the mixed layer within a few days to weeks following fertilization. Larvae in the upper ocean will be transported by faster and more dispersive currents [e.g., wind- and wave driven currents (Röhrs et al., 2012)] than those residing in deeper layers where currents are typically slower, primarily density driven and more topographically steered. Ontogenetic vertical migration, and a resulting drift at depths much shallower than those of spawning, has been confirmed for larvae of the deep-sea mussel *"Bathymodiolus" childressi* (Arellano et al., 2014). The observed pattern was suggested to explain genetic similarities across large geographical distances and biophysical modelling indicated that the depth of larval transport may indeed have a strong impact on dispersal (McVeigh et al., 2017). Analogous modelling results, as well as genetic data, have been documented for *L. pertusa* (Dahl, 2013; Fox et al., 2016), adding to the notion that effective vertical migration is a mechanism that may strongly impact larval dispersal for deep-sea species with an extensive planktonic phase.

Larvae spawned at shallow sites, such as those located in the North Sea and the Skagerrak, may spend a major part of their pre-competency period within the mixed layer. In this region, during spring when many larvae are likely to be pre-competent, the temperature tends to be lower within the mixed layer than deeper down. For these larvae, time spent in the upper ocean may consequently enhance their dispersal by speeding up their drift as well as by slowing down their development rate.

Following our findings, further detailed studies on the body composition, body density distribution and swimming mechanism in *L. pertusa* planulae would be of great value. Studies of larval body shape plasticity and possible associated responses to environmental conditions such as turbulence may also reveal highly interesting traits of ecological importance.

Our work has shown that pre-competent larvae of the cold-water coral *L. pertusa* maintain directed swimming in weak to moderate oceanic turbulence, thus allowing them to perform extensive vertical migration in their natural habitat. The mechanics behind the trait is however still to be explored and any future work on the topic would likely reveal information applicable to a wider range of larvae with similar morphology.

Conclusions

The grid-stirred tank constructed for this study produced turbulence with turbulent kinetic energy dissipation rates, ϵ, between 9.03×10^{-9} and 1.05×10^{-5} m^2 s^{-3}, quantified using particle image velocimetry (PIV). The span of dissipation rates was found to be appropriate for monitoring critical changes in vertical migration of pre-competent larvae of the cold-water coral *Lophelia pertusa*. Compared to experiments in still water, the upwards directed swimming speed was reduced by 22% in turbulence with $\epsilon \approx 10^{-8}$ m^2 s^{-3} and by 39% in turbulence with $\epsilon \approx 10^{-7}$ m^2 s^{-3}. In more intense turbulence ($\epsilon \geq 2.28 \times 10^{-6}$ m^2 s^{-3}) upwards directed swimming was no longer observed. Linking our experimental results to measurements of ϵ in various parts of the ocean (Fuchs and Gerbi, 2016; Bendtsen and Richardson, 2018; Franks et al., 2022), we conclude that *L. pertusa* planulae maintain upwards directed swimming in the open ocean away from boundaries. We further conclude that, for most of the oceanic water column, the vertical swimming velocities of larvae are likely reduced by< 20% compared to when swimming in still water.

Our results suggest that, despite the expectation of high sensitivity to turbulence, active vertical migration may allow *L. pertusa* larvae to spend a substantial part of their planktonic phase within the mixed layer. Residence in the upper parts of the ocean may expose larvae to environmental conditions much different from those encountered at spawning depth and may, consequently, have a significant effect on their dispersal. Such information about the vertical migration of larvae is essential for the development of biophysical larval transport models and is important for our understanding of population connectivity.

Data availability statement

The raw data supporting the conclusions of this article will be made available by the authors, without undue reservation.

Author contributions

AL and VF conceived the study and designed the experiments. GB contributed to the planning and materialization of the experimental work. AL managed the coral sampling as well as the coral rearing and larval culturing. AL arranged for the facilities as well as much of the material used. VF constructed the grid-stirred tank and performed most of the experimental work as well as the subsequent data analysis. AL contributed substantially to all steps of the experimental work, including data analyses. VF created all figures for the paper and wrote the original draft with substantial contribution from AL and GB. AL and GB supervised VF throughout all phases of the study. All authors contributed to the article and approved the submitted version.

Acknowledgment

We want to acknowledge the Oceanography Marks Foundation (Knut J:son Mark) at the University of Gothenburg for financial support of the first author's PhD studies. We also want to thank the Carl Trygger Foundation for funding the purchase of laboratory equipment used for the study (CTS 17:278).

Conflict of interest

The authors declare that the research was conducted in the absence of any commercial or financial relationships that could be construed as a potential conflict of interest.

Publisher's note

Supplementary material

The Supplementary Material for this article can be found online at: https://www.frontiersin.org/articles/10.3389/fmars.2022.1062884/full#supplementary-material

References

Arellano, S. M., Van Gaest, A. L., Johnson, S. B., Vrijenhoek, R. C., and Young, C. M. (2014). Larvae from deep-sea methane seeps disperse in surface waters. *Proc. R. Soc. B.* 281 (1786), 20133276. doi: 10.1098/rspb.2013.3276

Bendtsen, J., and Richardson, K. (2018). Turbulence measurements suggest high rates of new production over the shelf edge in the northeastern north Sea during summer. *Biogeosciences* 15, 7315–7332. doi: 10.5194/bg-15-7315-2018

Brooke, J., and Young, C. M. (2003). Reproductive ecology of a deep-water scleractinian coral, oculina varicosa, from the southeast Florida shelf. *Cont. Shelf. Res.* 23 (9), 847–858. doi: 10.1016/S0278-4343(03)00080-3

Clay, T. W., and Grünbaum, D. (2010). Morphology-flow interactions lead to stage-selective vertical transport of larval sand dollars in shear flow. *J. Exp. Biol.* 213 (8), 1281–1292. doi: 10.1242/jeb.037200

Dahl, M. (2013). *Conservation genetics of lophelia pertusa* (Gothenburg, Sweden: University of Gothenburg).

Fosså, J. H., Mortensen, P. B., and Furevik, D. M. (2002). The deep-water coral *Lophelia pertusa* in Norwegian waters: distribution and fishery impacts. *Hydrobiologia* 471 (1), 1–12. doi: 10.1023/A:1016504430684

Fox, A. D., Henry, L. A., Corne, D. W., and Roberts, J. M. (2016). Sensitivity of marine protected area network connectivity to atmospheric variability. *R. Soc Open Sci.* 3, 160494. doi: 10.1098/rsos.160494

Fox, J., and Weisberg, S. (2019). *An {R} companion to applied regression, third edition* (Thousand Oaks CA: Sage). Available at: https://socialsciences.mcmaster.ca/jfox/Books/Companion/.

Franks, P. J. S., Inman, B. G., MacKinnon, J. A., Alford, M. H., and Waterhouse, A. F. (2022). Oceanic turbulence from a planktonic perspective. *Limnol. Oceanogr* 67, 348–363. doi: 10.1002/lno.11996

Freiwald, A., Fosså, J. H., Grehan, A., Koslow, T., and Roberts, J. M. (2004). *Cold-water coral reefs* (Cambridge, UK: UNEP-WCMC).

Fuchs, H. L., and Gerbi, G. P. (2016). Seascape-level variation in turbulence- and wave-generated hydrodynamic signals experienced by plankton. *Prog. Oceanogr.* 141, 109–129. doi: 10.1016/j.pocean.2015.12.010

Fuchs, H. L., Gerbi, G. P., Hunter, E. J., Christman, A. J., and Diez, F. J. (2015). Hydrodynamic sensing and behavior by oyster larvae in turbulence and waves. *J. Exp. Biol.* 218 (9), 1419–1432. doi: 10.1242/jeb.118562

Fuchs, H. L., Hunter, E. J., Schmitt, E. L., and Guazzo, R. A. (2013). Active downward propulsion by oyster larvae in turbulence. *J. Exp. Biol.* 216 (8), 1458–1469. doi: 10.1242/jeb.079855

Fuchs, H. L., Mullineaux, L. S., and Solow, A. R. (2004). Sinking behavior of gastropod larvae (*Ilyanassa obsoleta*) in turbulence. *Limnol. Oceanogr.* 49 (6), 1937–1948. doi: 10.4319/lo.2004.49.6.1937

Gary, S. F., Fox, A. D., Biastoch, A., Roberts, J. M., and Cunningham, S. A. (2020). Larval behaviour, dispersal and population connectivity in the deep sea. *Sci. Rep.* 10, 10675. doi: 10.1038/s41598-020-67503-7

Gastwirth, J. L., Gel, Y. R., Hui, W. L. W., Lyubchich, V., Miao, W., and Noguchi, K. (2019) *Lawstat: Tools for biostatistics, public policy, and law. r package version 3.3.* Available at: https://CRAN.R-project.org/package=lawstat.

George, W. K., and Hussien, H. J. (1991). Locally axisymmetric turbulence. *J. Fluid. Mech.* 233, 1–23. doi: 10.1017/S0022112091000368

Grünbaum, D., and Strathmann, R. R. (2003). Form, performance and trade-offs in swimming and stability of armed larvae. *J. Mar. Res.* 61 (5), 659–691. doi: 10.1357/002224003771815990

Jonsson, P., Andre, C., and Lindegarth, M. (1991). Swimming behaviour of marine bivalve larvae in a flume boundary-layer flow: Evidence for near-bottom confinement. *Mar. Ecol.: Prog. Ser.* 79, 67–76. doi: 10.3354/meps079067

Kiørboe, T., and Saiz, E. (1995). Planktivorous feeding in calm and turbulent environments, with emphasis on copepods. *Mar. Ecol.: Prog. Ser.* 122, 135–145. doi: 10.3354/meps122135

Koslow, J. A., Gowlett-Holmes, K., Lowry, J. K., O'Hara, T., Poore, G. C. B., and Williams, A. (2001). Seamount benthic macrofauna off southern Tasmania: community structure and impacts of trawling. *Mar. Ecol.: Prog. Ser.* 213, 111–125. doi: 10.3354/meps213111

Larsson, A. I., Järnegren, J., Strömberg, S. M., Dahl, M. P., Lundälv, T., and Brooke, S. (2014). Embryogenesis and larval biology of the cold-water coral lophelia pertusa (A. davies, ed.). *PloS One* 9 (7), e102222. doi: 10.1371/journal.pone.0102222

Levin, L. A. (2006). Recent progress in understanding larval dispersal: new directions and digressions. *Integr. Comp. Biol.* 46, 282–297. doi: 10.1093/icb/icj024

McDonald, K. A. (2012). Earliest ciliary swimming effects vertical transport of planktonic embryos in turbulence and shear flow. *J. Exp. Biol.* 215 (1), 141–151. doi: 10.1242/jeb.060541

McVeigh, D. M., Eggleston, D. B., Todd, A. C., Young, C. M., and He, R. (2017). The influence of larval migration and dispersal depth on potential larval trajectories of a deep-sea bivalve. *Deep. Sea. Res. 1 Oceanogr. Res. Pap.* 127, 57–64. doi: 10.1016/j.dsr.2017.08.002

Meijering, E., Dzyubachyk, O., and Smal, I. (2012). Methods for cell and particle tracking. *Methods Enzymol.* 504, 183–200. doi: 10.1016/B978-0-12-391857-4.00009-4

R Core Team (2020). *R: A language and environment for statistical computing* (Vienna, Austria: R Foundation for Statistical Computing). Available at: https://www.R-project.org/.

Roberts, J. M. (2006). Reefs of the deep: The biology and geology of cold-water coral ecosystems. *Science* 312 (5773), 543–547. doi: 10.1126/science.1119861

Roberts, J. M., Long, D., Wilson, J. B., Mortensen, P. B., and Gage, J. D. (2003). The cold-water coral lophelia pertusa (Scleractinia) and enigmatic seabed mounds along the north-east Atlantic margin: Are they related? *Mar. pollut. Bull.* 46 (1), 7–20. doi: 10.1016/s0025-326x(02)00259-x

Roberts, J. M., Wheeler, A., Freiwald, A., and Cairns, S. D. (2009). *Cold-water corals: The biology and geology of deep-Sea coral habitats* (Cambridge: Cambridge University Press). doi: 10.1017/CBO9780511581588

Rogers, A. D. (1999). The biology of lophelia pertusa and other deep-water reef-forming corals and impacts from human activities. *Int. Rev. Hydrobiol.* 84 (4), 315–406. doi: 10.1002/iroh.199900032

Röhrs, J., Christensen, K. H., Hole, L. R., Broström, G., Drivdal, M., and Sundby, S. (2012). Observation-based evaluation of surface wave effects on currents and trajectory forecasts. *Ocean. Dynamics.* 62, 1519–1533. doi: 10.1007/s10236-012-0576-y

Saarenrinne, P., and Piirto, M. (2000). Turbulent kinetic energy dissipation rate estimation from PIV velocity vector fields. *Exp. Fluids.* 29, 300–307. doi: 10.1007/s003480070032

Sameoto, J. A., and Metaxas, A. (2008). Interactive effects of haloclines and food patches on the vertical distribution of 3 species of temperate invertebrate larvae. *J. Exp. Mar. Biol. Ecol.* 367, 131–141. doi: 10.1016/j.jembe.2008.09.003

Schneider, C. A., Rasband, W. S., and Eliceiri, K. W. (2012). NIH Image to ImageJ: 25 years of image analysis. *Nat. Methods* 9 (7), 671–675. doi: 10.1038/nmeth.2089

Strömberg, S. M., and Larsson, A. I. (2017). Larval behavior and longevity in the cold-water coral *Lophelia pertusa* indicate potential for long distance dispersal. *Front. Mar. Sci.* 4. doi: 10.3389/fmars.2017.00411

Strömberg, S. M., Östman, C., and Larsson, A. I. (2019). The cnidome and ultrastructural morphology of late planulae in *Lophelia pertusa* (Linnaeus 1758)–with implications for settling competency. *Acta Zool.* 100 (4), 431–450. doi: 10.1111/azo.12296

Tanaka, T., and Eaton, J. K. (2007). A correction method for measuring turbulence kinetic energy dissipation rate by PIV. *Exp. Fluids.* 42, 893–902. doi: 10.1007/s003480070032

United Nations (2006). *Resolution adopted by the general assembly 61/105. sustainable fisheries, including through the 1995 agreement for the implementation of the provisions of the united nations convention on the law of the Sea of 10 December 1982 relating to the conservation and management of straddling fish stocks and highly migratory fish stocks, and related instruments* (New York: United Nations).

Wheeler, J. D., Chan, K. Y. K., Anderson, E. J., and Mullineaux, L. S. (2016). Ontogenetic changes in larval swimming and orientation of pre-competent sea urchin *Arbacia punctulata* in turbulence. 219 (9), 1303–1310. doi: 10.1242/jeb.129502

Wheeler, J. D., Helfrich, K. R., Anderson, E. J., McGann, B., Staats, P., Wargula, A. E., et al. (2013). Upward swimming of competent oyster larvae *Crassostrea virginica* persists in highly turbulent flow as detected by PIV flow subtraction. *Mar. Ecol.: Prog. Ser.* 488, 171–185. doi: 10.3354/meps10382